Received: 13 April 2020 | Accepted: 11 August 2020

DOI: 10.1111/gcb.15336

PRIMARY RESEARCH ARTICLES

Global Change Biology WILEY

Global variation in diurnal asymmetry in temperature, cloud cover, specific humidity and precipitation and its association with leaf area index

Daniel T. C. Cox | Ilya M. D. Maclean | Alexandra S. Gardner | Kevin J. Gaston

Environment and Sustainability Institute, University of Exeter, Penryn, UK

Correspondence
Daniel T. C. Cox, Environment and Sustainability Institute, University of Exeter, Penryn, Cornwall TR10 9FE, UK.
Email: d.t.c.cox@exeter.ac.uk

Funding information
Natural Environment Research Council, Grant/Award Number: NE/P01156X/1 and NE/P01229/1

Abstract

The impacts of the changing climate on the biological world vary across latitudes, habitats and spatial scales. By contrast, the time of day at which these changes are occurring has received relatively little attention. As biologically significant organismal activities often occur at particular times of day, any asymmetry in the rate of change between the daytime and night-time will skew the climatic pressures placed on them, and this could have profound impacts on the natural world. Here we determine global spatial variation in the difference in the mean annual rate at which near-surface daytime maximum and night-time minimum temperatures and mean daytime and mean night-time cloud cover, specific humidity and precipitation have changed over land. For the years 1983–2017, we derived hourly climate data and assigned each hour as occurring during daylight or darkness. In regions that showed warming asymmetry of >0.5°C (equivalent to mean surface temperature warming during the 20th century) we investigated corresponding changes in cloud cover, specific humidity and precipitation. We then examined the proportional change in leaf area index (LAI) as one potential biological response to diel warming asymmetry. We demonstrate that where night-time temperatures increased by >0.5°C more than daytime temperatures, cloud cover, specific humidity and precipitation increased. Conversely, where daytime temperatures increased by >0.5°C more than night-time temperatures, cloud cover, specific humidity and precipitation decreased. Driven primarily by increased cloud cover resulting in a dampening of daytime temperatures, over twice the area of land has experienced night-time warming by >0.25°C more than daytime warming, and has become wetter, with important consequences for plant phenology and species interactions. Conversely, greater daytime relative to night-time warming is associated with hotter, drier conditions, increasing species vulnerability to heat stress and water budgets. This was demonstrated by a divergent response of LAI to warming asymmetry.

KEYWORDS

activity patterns, climate change asymmetry, daytime warming, leaf area index, night-time warming, vegetation cover, warming asymmetry, water cycle

1 | INTRODUCTION

Human activities are altering the planet's climate, with biologically meaningful changes taking place from the macro- (IPCC, 2013) to the microscale (e.g. Maclean, Suggitt, Wilson, Duffy, & Bennie, 2017; Suggitt et al., 2018). Anthropogenic increases in atmospheric CO_2 and other greenhouse gases have resulted in a strong global trend of increasing maximum and minimum temperatures (IPCC, 2013), which in turn has driven an intensification of the hydrological cycle (e.g. Huntington, 2006; Ohmura & Wild, 2002). The rates and directions in which these changes are occurring have been shown to vary with land use and land cover change (e.g. Pielke, 2005), across elevations (e.g. Rangwala, Sinsky, & Miller, 2013), ecoregions (e.g. Beaumont et al., 2011; Zhou, Chen, & Dai, 2015) and latitudes (e.g. Deutsch et al., 2008), and the associated impacts of these changes on the natural world have been diverse (e.g. Maclean & Wilson, 2011; Walther et al., 2002). By contrast with the rich literature examining spatial variation in climate change, that exploring temporal variation focuses principally on changes to daily, monthly, or annual means. Variation in the rates at which these changes are occurring across the diel (daily) cycle has received surprisingly little attention. However, if the climate is not changing at a consistent rate during both the daytime and night-time, then the use of daily means will lead to underestimation or overestimation of changes across a particular dimension of the day. Given that many species show strong time partitioning in their daily biological processes (e.g. plant photosynthesis; Xu, Medvigy, Powers, Becknell, & Guan, 2016) or activity patterns (Bennie, Duffy, Inger, & Gaston, 2014), neglecting sub-daily changes in climate could have important consequences for predicting the impacts of climate change on global biodiversity.

There has been a global trend of night-time temperatures increasing at a faster rate than daytime temperatures (Davy, Esau, Chernokulsky, Outten, & Zilitinkevich, 2017; Easterling et al., 1997; Karl et al., 1991; Vose, Easterling, & Gleason, 2005), which has led to a shrinking of the diel temperature range (e.g. Vose et al., 2005). This diel asymmetry in warming varies spatially, with some regions also experiencing daytime temperatures increasing faster than night-time temperatures (Donat & Alexander, 2012; Easterling et al., 1997). The downward trend in daily temperature ranges is thought ultimately to be related to the upward trend in cloud cover over land (Dai, Genio, & Fung, 1997; Dai, Trenberth, & Karl, 1999; Sun, Groisman, Bradley, & Keimig, 2000), with clouds having a strong and opposing effect on temperature, dependent on the time of day (Sun et al., 2000). During the daytime, clouds attenuate shortwave radiation resulting in a lowering of daytime temperatures, whilst at night they re-emit longwave radiation downward, warming the earth's surface (Dai et al., 1999). Warming asymmetry has also been attributed to soil moisture (Dai et al., 1999), precipitation (Dai et al., 1997; Zhou et al., 2009), boundary layer depth (Davy et al., 2017) and at smaller spatial scales, anthropogenic land forcing (e.g. Chen & Dirmeyer, 2019; Lee et al., 2011).

Rising temperatures are associated with increased evapotranspiration that has been attributed to global trends of increasing cloud cover and near-surface humidity and precipitation (e.g. Huntington, 2006; Ohmura & Wild, 2002), further influencing daily temperature ranges (e.g. Dai et al., 1999; Du, Wu, Jin, Zong, & Meng, 2013; Zhou et al., 2015). Because a warmer atmosphere is able to hold more moisture, one might predict that asymmetric warming may impact cloud cover, specific humidity and precipitation differently at different times of the day. Consequently, in regions where the night-time is warming faster than the daytime we may expect to see greater relative increases in night-time specific humidity than daytime specific humidity owing to the temperature-dependent limits on how much water vapour a given volume of air can hold (Gaffen & Ross, 1999; Wang & Gaffen, 2001). Conversely, relatively higher temperatures during the daytime potentially enable more moisture to be held in the atmosphere, which can lead to increased levels of specific humidity and precipitation during the daytime.

As biological activities and processes often occur at particular times of day, diel asymmetries in warming, cloud cover, humidity or precipitation are likely to have diverse and profound consequences for the natural world. In plants, for example, rising minimum night-time temperatures are expected to affect carbon assimilation and consumption, because most photosynthesis occurs during the daytime and is more sensitive to maximum daytime temperatures, whereas respiration occurs throughout the diel cycle (Atkin et al., 2013) and is influenced by both daytime maximum and night-time minimum temperatures (Peng et al., 2013; Peraudeau et al., 2015; Xia et al., 2014). Night-time warming has been found to affect vegetation growth (Alward, Detling, & Milchunas, 1999; Peng et al., 2004, 2013; Xia et al., 2014), however, responses of vegetation to diel asymmetric warming differ between regions and ecosystems (Alward et al., 1999; Beier et al., 2008; Peng et al., 2004, 2013; Wan, Xia, Liu, & Niu, 2009) and large-scale responses are less clear. In the Northern Hemisphere, positive correlations have been observed between daytime maximum temperatures and vegetation growth in wet and cool ecosystems, but negative correlations in dry temperate regions (Peng et al., 2013). However, global trends in changing vegetation cover in response to warming asymmetry are not currently known.

Studies to date investigating diel asymmetry in warming have been hampered by incomplete spatial coverage (e.g. Easterling et al., 1997; Karl et al., 1993; Vose et al., 2005) or have tended to focus on a specific hemisphere (e.g. Davy et al., 2017; Peng et al., 2013) or region (e.g. Kuang & Jiao, 2016). Moreover, it is not known whether diel warming asymmetry is matched by diurnal asymmetry in other climate variables such as cloud cover, specific humidity or precipitation. Globally, it is currently unclear how diurnal asymmetry in the changing climate varies spatially, where the extreme differences between daytime and night-time warming are taking place, and what proportion of the land's surface is undergoing different rates of warming.

Here we use a 35 year global data set for near-surface temperature, cloud cover, specific humidity and precipitation to examine: (a)

associations between the long-term trend in mean daily cloud cover and the difference in the rate of change between daytime maximum temperatures and night-time minimum temperatures; (b) spatial variation in the difference in the rate of change between mean daytime and mean night-time cloud cover, specific humidity and precipitation; (c) the relationship between warming asymmetry and diurnal asymmetry in cloud cover, specific humidity and precipitation in regions that have experienced a greater increase of >0.5°C in the daytime or the night-time; and (d) climate change asymmetry in three case study regions that display high degrees of warming asymmetry, namely the Tibetan Plateau, West Africa and East Africa. Finally, (e) we examine one potential biological response to diel warming asymmetry, change over recent decades in vegetation cover (measured through the leaf area index; LAI).

2 | METHODS

We used NCEP Reanalysis 2 climate data provided by the NOAA/OAR/ESRL PSD (https://www.esrl.noaa.gov/psd/). This is a global gridded data set of modelled forecasts and hindcasts calibrated against observed data and is the best long-term reanalysis data set currently available. All spatial manipulations were performed in QGIS v3.4 (QGIS Development Team, 2018) and R software for statistical computing v3.5.2 (R Core Team, 2018). We used the R packages 'microclima' (Maclean, Mosedale, & Bennie, 2019) for data preparation and 'raster' (Hijmans, 2019) for raster manipulation.

We downloaded near-surface 6 hourly observations for temperature (°C) at 2 m above ground level, cloud cover (%), specific humidity (g/m^3) and the precipitation rate at the surface (mm). We used specific humidity instead of relative humidity to avoid conflation with temperature. Data were from 1983 to 2017 and recorded at 1.904 × 1.875 degree resolution. The data set covered from 89.5°N to 89.5°S and was projected using WGS84. A spline interpolation was then used to produce hourly climate estimates for cloud cover and specific humidity. For temperature, a more sophisticated interpolation was used in which this is assumed to follow a sinusoidal diurnal cycle, with the periodicity determined by sunrise and sunset. Final values for temperature were then calculated using the 'hourlytemp' function in the R package 'microclima' where deviations from this cycle are determined by daytime solar radiation and night-time sky emissivity. The 'suntimes' function provided the time of sunrise and sunset for the centroid of each pixel, allowing a binary raster for each hour of the day to be generated showing whether this was during the daytime or night-time (rounded to the nearest hour). The ocean exerts different pressures on the climate compared to the land (Sutton, Suckling, & Hawkins, 2015), therefore for all climate variables we masked pixels where the ocean covered the centroid of the pixel. We also excluded small islands. For precipitation, for which estimates are provided over a 6 hr period, amounts were partitioned according to whether more than half of day or night fell within the 6 hr period. Finally, to avoid giving undue weighting to pixels at high latitudes for each year, we reprojected the rasters for each climate variable to the Behrmann equal area projection (181 × 243 km resolution; EASE-Grid 2.0: EPSG:6933; Brodzik, Billingsley, Haran, Raup, & Savoie, 2012).

2.1 | Daytime and night-time climate trends

In each terrestrial pixel for every 24 hr cycle, we determined the maximum daytime temperature and the minimum night-time temperature, before taking the mean across each year. We focused on daytime maximum and night-time minimum temperature, because we were interested in the ecological impacts of changing extremes of daytime and night-time temperature variation that have been shown to have greater ecological impacts than temperature means (Ma, Hoffmann, & Ma, 2015). Unlike temperature, cloud cover, specific humidity and precipitation do not follow a similar consistent daily cycle, and so we examined long-term trends in annual mean daytime and annual mean night-time measures. Higher latitudes experience 24 hr daylight and darkness and so diel asymmetry is conflated with seasonal asymmetry, and we therefore excluded 24 hr periods that were solely day or night. To obtain a global average for each climate variable in each year for the daytime and again for the night-time we calculated the mean value across pixels. We then built a linear model of the annual global anomaly relative to the 35 year mean for daytime and night-time (response) modelled first against year (0–34) and then against the interaction between year and a binary factor of daytime and night-time. As a measure of the level of variation explained by the linear regression, for each model we also calculated McFadden's pseudo *R*-squared.

To understand the spatial distribution of diel warming asymmetry, for each year for the daytime and again for the night-time, we carried out linear regression across years for each pixel before multiplying the slope by 35 years to calculate the absolute level of warming between 1983 and 2017. To calculate the difference in the rate of change between the daytime and the night-time, we subtracted the daytime change from the night-time change. We then repeated this process for cloud cover, specific humidity and precipitation. To capture the area of land experiencing greater change in the daytime or the night-time, we calculated the percentage of land that crossed an arbitrary asymmetry threshold, namely temperature >0.25°C, cloud cover >2.5%, specific humidity >0.1 g/m^3 and precipitation >0.1 mm. Finally, we plotted the daytime and night-time annual global anomalies against the long-term means.

Cloud cover has a strong influence on surface solar heating and upward longwave radiation (Dai et al., 1997; Sun et al., 2000), therefore we examined the relationship between mean daily cloud cover and the temperature change difference between day and night. For each pixel and year as above, we calculated the mean daily cloud cover before carrying out linear regression across years for each

pixel to determine the level of cloud cover change between 1983 and 2017. We then calculated Pearson's correlation between the diel temperature change difference and (a) mean daily cloud cover, (b) diel cloud clover change difference, (c) diel specific humidity change difference, and (d) diel precipitation change difference.

To explore the relationship between diel warming asymmetry and diurnal differences in the rate of change of cloud cover, specific humidity and precipitation, for each climate variable we selected all pixels that experienced: (a) night-time minimum warming of >0.5°C more than the daytime maximum, and (b) daytime maximum warming of >0.5°C more than the night-time minimum (0.5°C being the level that the mean surface air temperature warmed during the 20th century; IPCC, 2013). For the daytime and night-time we then plotted the global anomaly against the long-term mean.

To understand the relationship between warming asymmetry and diel asymmetry in cloud cover, specific humidity and precipitation at smaller spatial scales, which may be influenced by different processes and pressures, we examined climate asymmetry in three case study regions that displayed high levels of warming asymmetry (e.g. Pingale, Adamowski, Jat, & Khare, 2015): (a) the Tibetan Plateau, a high altitude site that has experienced high levels of night-time warming and has been the focus of intense climate research; and two tropical regions that experienced asymmetry in, respectively, the night-time (b) West Africa, and the daytime (c) East Africa. At each site for the daytime and the night-time we plotted the global anomaly against the long-term mean.

2.2 | The response of vegetation cover to warming asymmetry

To examine a biological response to the 35 year change in warming asymmetry, we quantified relationships with the $\log_e$ proportional change in LAI. LAI is the total one-sided leaf area per unit ground area and therefore a strong indicator of volumetric biomass within an ecosystem and is a critical variable scaling photosynthesis, respiration and evapotranspiration (Asner, Braswell, Schimel, & Wessman, 1998; Boussetta, Balsamo, Beljaars, Kral, & Jarlan, 2013; Jarlan et al., 2008). A daily 0.05° gridded data set (1983–2017) of LAI values was downloaded from the National Climatic Data Center (Vermote & NOAA CDR Program, 2019). Values were then averaged for each month. Missing values from regions obscured by cloud cover, or not obtained due to adverse data capture conditions were imputed as follows. First, the entire globe was divided into 100, 36° × 18° regions. Within each region mean values for each month were calculated, and all grid cells values were divided by the mean monthly value. Missing values were then approximated by spline interpolation on the time series for each grid cell, before multiplying by the mean monthly value to add the seasonal effect back in. This, in effect, removes the season effect before interpolation so as to ensure that if missing values coincided with seasonal peaks or troughs in LAI, values are not over- or underestimated. For a small number of locations with a high proportion of missing data, LAI values could not be estimated in this way. For these locations, a land cover type was identified using a data set from the European Space Agency (Lamarche et al., 2017). Grid cells were then assigned the mean monthly value of LAI for that land cover type, estimated using non-missing data and separately for each 36 × 18° region.

Data were aggregated in annual composites of mean LAI, before being reprojected to the Behrmann equal area projection and resampled to match the resolution of the equal area climate layers (181 × 243 km). For each land pixel, we carried out linear regression across years before calculating the total $\log_e$ proportional change in LAI between 1983 and 2017. We then modelled the $\log_e$ proportional change in LAI (response) against the interaction between the absolute change in total annual precipitation and a binary factor of whether warming occurred more during the daytime or the night-time. The absolute change in precipitation in each pixel was determined as the linear regression of the total annual precipitation in each pixel multiplied by 35 years.

3 | RESULTS

Global trends did not reveal diurnal asymmetry in the annual rate at which daytime maximum and night-time minimum near-surface temperatures, and mean daytime and mean night-time cloud cover, specific humidity and precipitation have changed over land between 1983 and 2017 (Table 1; Figures 1 and 2). However, there

Variable	Dimension	Coefficient	Total change	pR^2
Temperature (°C)	Year	0.029 (0.002)***	1.02	
	Day/Night	0.004 (0.004)	0.14	.72
Cloud cover (%)	Year	6.9e-3 (0.005)	0.24	
	Day/Night	−6.4e-4 (0.01)	−0.02	.12
Specific humidity (g/m^3)	Year	0.013 (0.0013)***	0.46	
	Day/Night	−0.0013 (0.0026)	0.046	.59
Precipitation (mm/6 hr)	Year	0.0014 (2.5e-4)**	0.05	
	Day/Night	−2.9e-4 (5.2e-4)	−0.01	.34

Note: Statistical significance is shown as: **<.01; ***<.001. The pR^2 is McFaddon's.

TABLE 1 Global trends in the annual rate at which maximum daytime and minimum night-time temperature, and mean cloud cover, specific humidity and precipitation have changed over land between the daytime and the night-time. Year shows the 35 year trend for the daytime and night-time, Day/Night gives the interaction between year and a binary variable of day and night

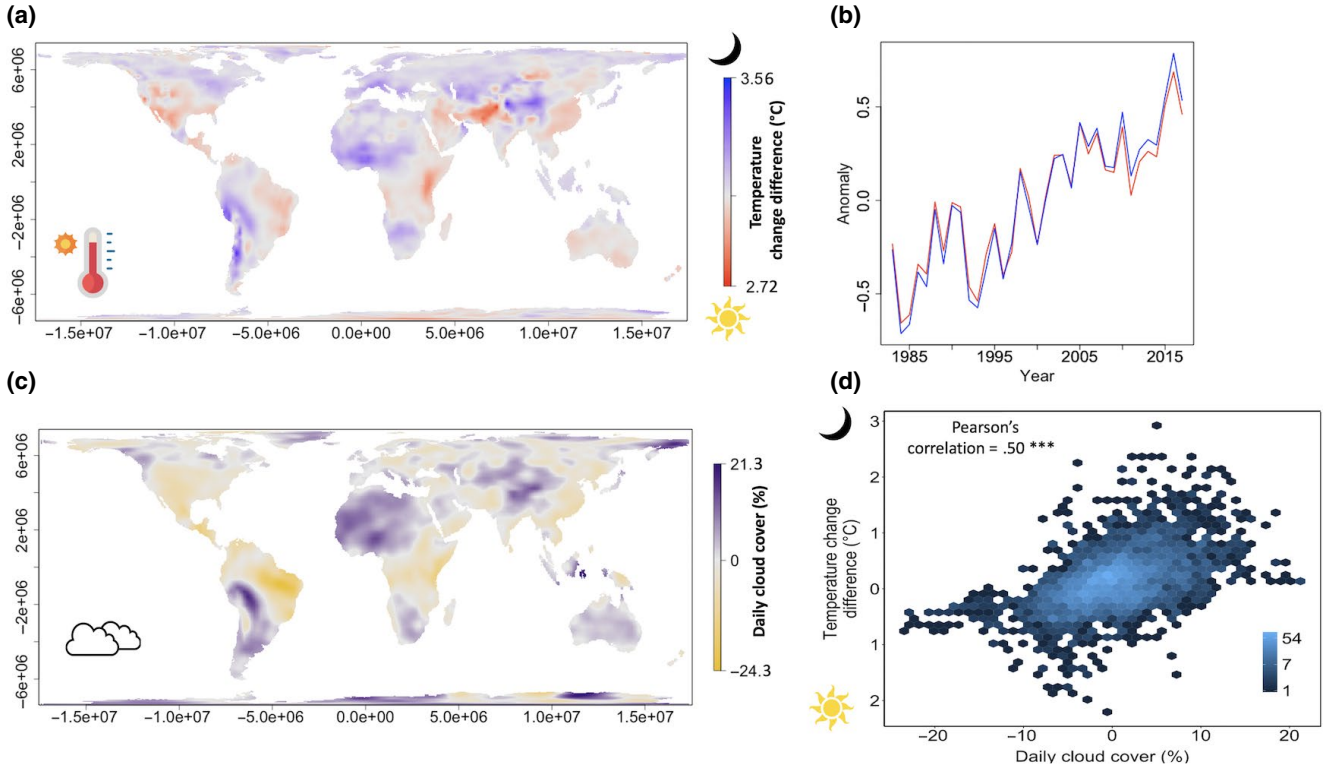

FIGURE 1 Spatial variation in diel warming asymmetry and change in daily cloud cover. (a) Spatial variation in the warming asymmetry between daytime maximum temperature and night-time minimum temperature. In each pixel the 35 year change in the daytime temperature was subtracted from the 35 year change in the night-time temperature. Red illustrates where the daytime has changed more rapidly and blue where the night-time has done so. (b) Anomaly plot of annual mean daytime maximum temperature (red) and annual mean night-time minimum temperature (blue) relative to the 35 year mean. (c) Spatial variation in cloud cover change. Pixels show the 35 year trend in mean daily cloud cover where yellow illustrates where cloud cover has decreased and purple where cloud cover has increased. (d) The relationship between the difference in change in temperature between the daytime and night-time and the change in daily cloud cover. The legend shows the log of the number of pixels, and *** denotes a statistical significance of $p < .001$. Negative values for temperature change difference were converted to absolute values and the direction of greater change is represented by a sun (daytime) or a moon (night-time). The map projections are Behrmann's equal area

was significant spatial variation in the degree to which all variables have changed across the diel cycle (Table 2; Figures 1 and 2). The 35 year trend in mean daily cloud cover was correlated with the temperature change difference between daytime maximum and night-time minimum temperatures (Pearson's correlation = .50; Figure 1d), with regions where cloud cover has increased showing a trend of greater night-time warming and regions where cloud cover has decreased showing a trend of greater daytime warming (Figure 1).

Over twice the area of land has experienced increased warming at night of >0.25°C relative to the daytime, whereas similar areas of land saw changes in cloud cover of >2.5% across the daytime or the night-time (Table 2; Figures 1 and 2). Globally, over twice the area of land has experienced increased specific humidity >0.1 g/m^3 during the daytime than the night-time (Table 2; Figure 1), whilst increased rainfall of >0.1 mm/6 hr during the daytime has been more common than during the night-time. Although statistically significant, temperature change difference was less strongly correlated with cloud cover change difference and precipitation change difference (Pearson's correlation < .1), whilst specific humidity change difference was correlated with temperature change difference (Pearson's correlation = .35; Table 2; Figure 2aiii–ciii).

In those regions that experienced an increase of >0.5°C more at night than during the day there was a trend of increased levels of cloud cover, specific humidity and precipitation during the daytime and night-time (Table 3a; Figure 3a). Conversely, regions that underwent an increase of >0.5°C more during the daytime than the night-time experienced reduced levels of cloud cover, specific humidity and precipitation in both the daytime and night-time (Table 3b; Figure 3b).

At smaller spatial scales, the Tibetan Plateau has experienced median night-time minimum temperature increases of 1.2°C (range: 0.21°C; 3.44°C) more than daytime maximum temperatures, and this has been accompanied by increases in daytime and even greater increases in night-time cloud cover (Table 3c; Figure 4a). We found that specific humidity increased more in the daytime than the night-time, and there was some evidence that night-time precipitation has increased more quickly than daytime precipitation (Table 3c; Figure 4a). In West Africa there has been a median temperature change difference of night-time minimum temperatures increasing 0.95°C (range: 0.15°C; 2.12°C) more than

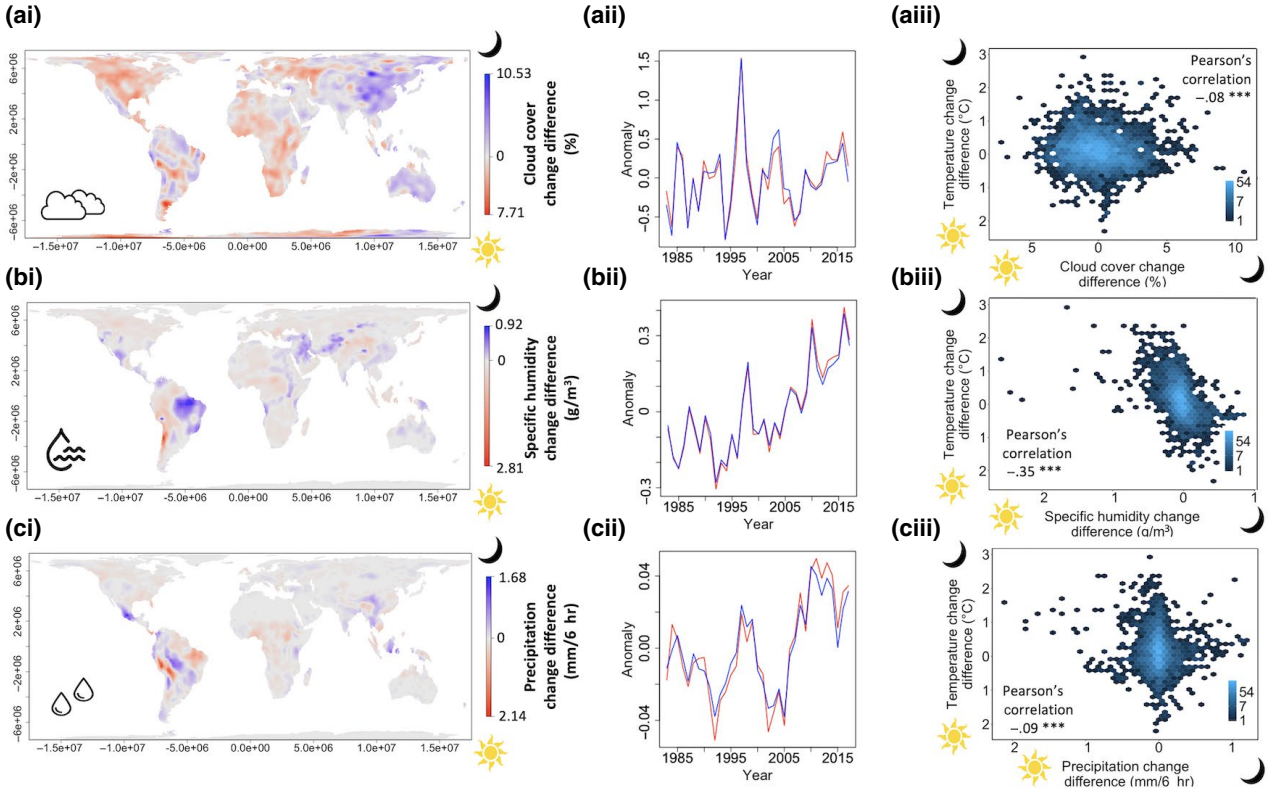

FIGURE 2 Spatial variation in diel asymmetry in cloud cover, specific humidity and precipitation. We show spatial variation in asymmetry between mean daytime and mean night-time (a) cloud cover (%), (b) specific humidity (g/m^3), and (c) precipitation (mm/6 hr). (ai, bi, ci) In each pixel the 35 year change in the daytime was subtracted from the 35 year change in the night-time. Red illustrates where the daytime has changed more rapidly and blue where the night-time has changed more rapidly. (aii, bii, cii) Anomaly plots of annual mean daytime (red) and annual mean night-time (blue) relative to the 35 year mean. (aiii, biii, ciii). The relationship between the difference in change in temperature between the daytime maximum and night-time minimum and the change difference between the mean daytime and mean night-time climate variable. The legend shows the log of the number of pixels, and *** denotes a statistical significance of $p < .001$. Negative values for the change difference were converted to absolute values and the direction of greater change is represented by a sun (daytime) or a moon (night-time). Therefore, a negative correlation in (iii) illustrates that greater night-time warming is associated with greater change in the climate variable during the daytime, while higher daytime temperatures are associated with greater change in the climate variable during the night-time. The map projections are Behrmann's equal area

TABLE 2 Spatial variation in diel asymmetry of temperature, cloud cover, specific humidity and precipitation. We show the mean annual difference in daytime maximum temperature and night-time minimum temperature and mean annual difference between mean daytime and mean night-time cloud cover, specific humidity and precipitation. A negative symbol for the median and interquartile range denotes that globally there was greater change in the daytime than the night-time

Variable	Median	Interquartile range	Daytime extreme (%)	Night-time extreme (%)	Correlation with warming asymmetry[a]	Daytime % land cover > threshold	Night-time % land cover > threshold
Cloud cover (%)							
Daily mean	0.8	−2.2; 5.2	−24.3	21.4	0.35	–	–
Temperature (°C)						Threshold > 0.25°C	
Nt_{min}–DY_{max}	0.07	−0.20; 0.34	2.72	3.56	–	17.7	36.6
Cloud cover (%)						Threshold > 2.5%	
Nt_{mean}–DY_{mean}	−0.14	−1.256; 1.03	7.17	10.53	−0.09	7.1	8.8
Specific humidity (g/m^3)						Threshold > 0.1 g/m^3	
Nt_{mean}–DY_{mean}	−0.037	−0.11; 0.013	2.81	0.92	−0.45	27.3	11.1
Precipitation (mm/6 hr)						Threshold > 0.1 mm/6 hr	
Nt_{mean}–DY_{mean}	−0.0054	−0.052; 0.03	2.14	1.68	−0.09	15.8	11.1

[a]The different rate of change between daytime maximum temperatures and night-time minimum temperatures.

TABLE 3 Diurnal asymmetry in temperature, cloud cover, specific humidity and precipitation. We selected all pixels that experienced warming of (a) >0.5°C in the daytime, (b) >0.5°C in the night-time, (c) the Tibetan Plateau, (d) West Africa and (e) East Africa. We show the parameter estimates and standard errors of two linear regressions, the first of the yearly anomaly for daytime and night-time (response) modelled against year (Year) and the second the yearly anomaly for daytime and night-time against the interaction between year and a binary factor of day/night (Day/Night). A negative result for Year indicates that the climate variable is decreasing. A negative result for Day/Night shows that the daytime is changing more rapidly than the night-time

Variable	(a) >0.5°C Daytime	(b) >0.5°C Night-time	(c) Tibetan Plateau	(d) West Africa	(e) East Africa
Lat/Lon	—	—	33°N, 88°E	09°N, 02°E	05°S, 36°E
Land area (km^2)	9,533,000	26,067,000	1,905,000	5,080,000	3,064,000
Temperature (°C)					
Year	**0.04 (0.03)*** **	**0.02 (0.003)*** **	−6.8e-4 (6.6e-3)	**0.009 (0.004)***	**0.03 (0.004)*** **
Year × Day/Night	**−0.03 (0.005)*** **	**0.03 (0.005)*** **	**0.037 (0.013)****	**0.028 (8e-3)*** **	**−0.016 (0.007)***
Cloud cover (%)					
Year	**−0.006 (6e-4)*** **	**0.06 (3.9e-4)*** **	**0.20 (0.02)*** **	**0.19 (0.02)*** **	**−0.20 (0.02)*** **
Year × Day/Night	−2.5e-4 (0.002)	−1.3e-3 (7.8e-4)	**0.08 (0.03)***	−0.04 (0.04)	−0.03 (0.04)
Specific humidity (g/m^3)					
Year	**−0.007 (0.003)***	**0.03 (0.001)*** **	**0.02 (0.002)*** **	**0.07 (0.004)*** **	**−0.015 (0.004)****
Year × Day/Night	0.003 (0.005)	−0.005 (0.003)	**−0.01 (0.003)****	−3.4e-3 (7.8e-3)	−3.3e-4 (9.0e-3)
Precipitation (mm/6 hr)					
Year	**−5.5e-3 (6.3e-4)****	**0.006 (3.9e-4)****	**0.003 (4.6e-4)*** **	**0.009 (0.001)*** **	**−0.01 (0.001)*** **
Year × Day/Night	−2.5e-4 (1.3e-3)	0.001 (7.8e-4)	0.002 (0.0009)$^{\#}$	−2.8e-3 (2.1e-3)	7.3e-4 (2.2e-3)

Note: Significant results are shown in bold.

Statistical significance is shown as: $^{\#}$<.06; *<.05; **<.01; ***<.001.

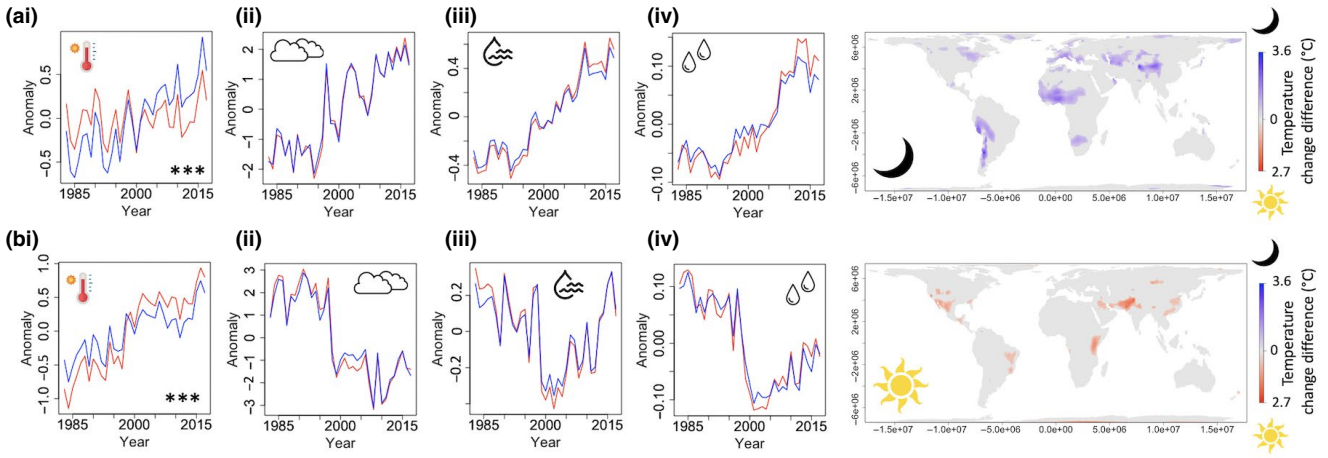

FIGURE 3 Diel asymmetry in the changing climate at extremes of >0.5°C warming asymmetry. We show the relationship between warming asymmetry and diurnal asymmetric change in cloud cover, specific humidity and precipitation, in regions where (a) the night-time minimum temperature warmed by >0.5°C more than the daytime maximum temperature, and (b) the daytime maximum temperature warmed by >0.5°C more than the night-time minimum temperature. We give the anomaly plots for of annual mean daytime (red) and annual mean night-time (blue) relative to the 35 year mean of (i) temperature (°C), (ii) cloud cover (%), (iii) specific humidity (g/m^3) and (iv) precipitation (mm/6 hr). *** denotes a statistical significance of the interaction between year and a binary day/night variable as $p < .001$. The global map was created by subtracting the change in daytime maximum temperature from the change in night-time minimum temperature, and masking regions where the warming threshold of >0.5°C was not met. Coloured areas illustrate where warming of >0.5°C that has occurred more in the daytime (red) or the night-time (blue). Negative values for temperature change difference were converted to absolute values and the direction of greater change is represented by a sun (daytime) or a moon (night-time). The map projections are Behrmann's equal area

daytime maximum temperatures, and this has been combined with equal increases in cloud cover, specific humidity and precipitation across the daytime and night-time (Table 3d; Figure 4b). In East Africa there has been a median temperature change difference of daytime maximum temperatures increasing 0.37°C (range: 0.05°C; 1.16°C) more than night-time minimum temperatures, and

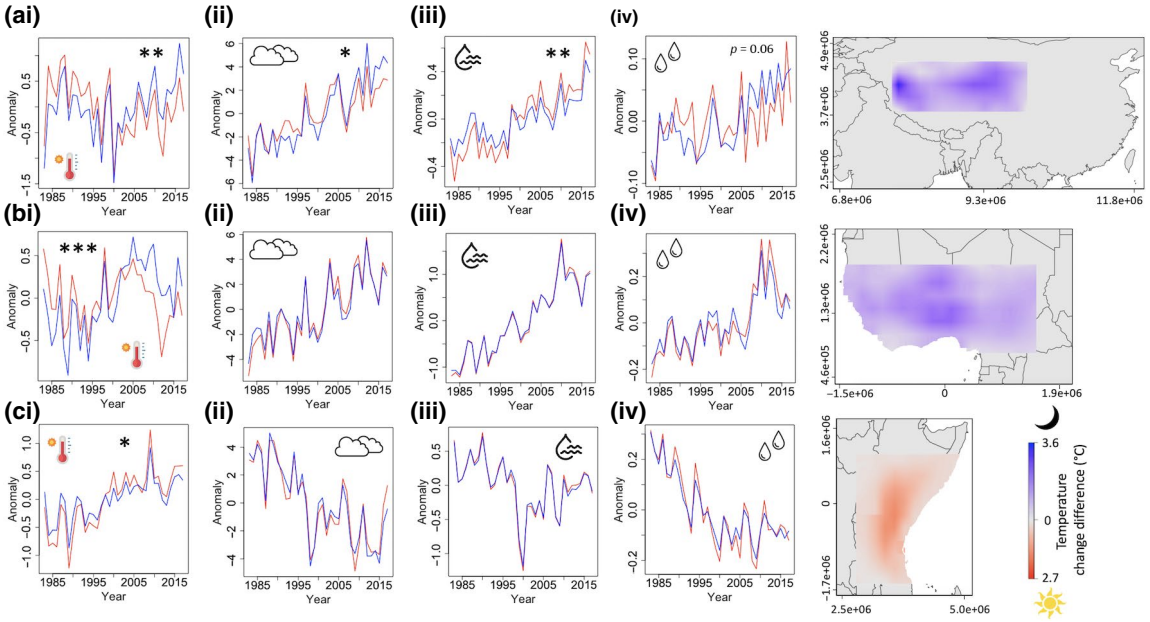

FIGURE 4 Diel asymmetry in the changing climate at smaller spatial scales. Warming asymmetry and diurnal asymmetric change in cloud cover, specific humidity and precipitation in (a) the Tibetan Plateau (33°N, 88°E), (b) West Africa (09°N, 02°E) and (c) East Africa (05°S, 36°E). We show the anomaly plots for annual mean daytime (red) and annual mean night-time (blue) relative to the 35 year mean of (i) temperature (°C), (ii) cloud cover (%), (iii) specific humidity (g/m^3) and (iv) precipitation (mm/6 hr). Statistical significance of the interaction between year and a binary day/night variable are shown as; *$p < .05$; **$p < .01$; ***$p < .001$. The global map was created by subtracting the change in daytime maximum temperature from the change in night-time minimum temperature. Coloured areas demarcate the degree to which the days warmed more quickly (red) or the nights warmed more quickly (blue). Negative values for temperature change difference were converted to absolute values and the direction of greater change is represented by a sun (daytime) or a moon (night-time). The map projections are Behrmann's equal area

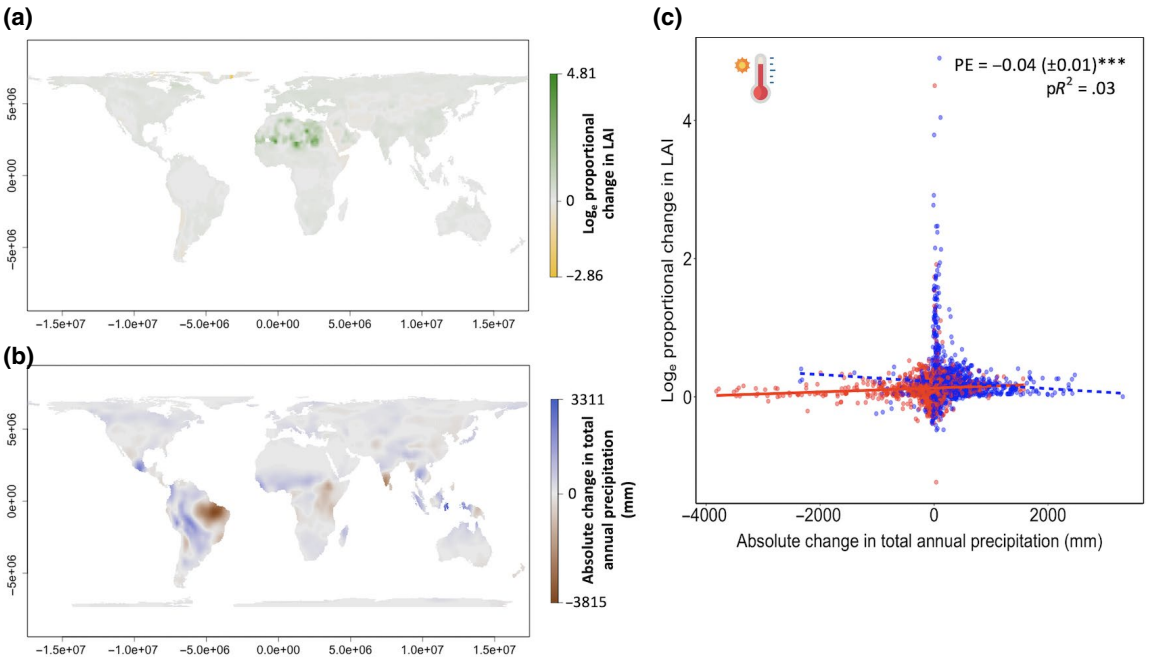

FIGURE 5 The response of LAI to diel warming asymmetry and absolute change in precipitation. We show spatial variation in (a) the log$_e$ proportional change in LAI between 1983 and 2017, and (b) the absolute change in total annual precipitation for the same period. (c) Relationship between the log$_e$ proportional change in LAI and the interaction between the absolute change in total annual precipitation and a binary factor of whether warming occurred more during the daytime (red) or the night-time (blue). We give the linear lines of best fit for the daytime (red, solid) and the night-time (blue, dashed), and the parameter estimate (PE) and standard error for the interaction. *** denotes a statistical significance of $p < .0001$. The pR^2 is McFaddon's. The map projections are Behrmann's equal area

this has been associated with equal decreases in cloud cover, specific humidity and precipitation during the daytime and night-time (Table 3e; Figure 4c).

Globally, there was a trend for increasing LAI between 1983 and 2017, but with significant spatial variation (median $\log_e$ proportional change = 0.15; range: −2.93; 4.90; Figure 5a). There was also significant variation in the absolute change in annual precipitation for the same period (Figure 5b). In those regions that experienced greater night-time warming, there was a negative association between precipitation and LAI, whilst in those regions that experienced greater daytime warming precipitation was positively associated with LAI (Figure 5c).

4 | DISCUSSION

We demonstrate that diurnal asymmetry in the changing climate primarily occurs in the differing rates of change in near-surface temperatures, and provide evidence that this is largely driven by changing levels of mean daily cloud cover. Overall, we found that more land has experienced greater night-time warming than has experienced greater daytime warming, and that this has been accompanied by increased cloud cover, specific humidity and precipitation. Conversely, regions where greater daytime warming has taken place have experienced twice the levels of overall warming and this was combined with reduced cloud cover and a drying of the climate. Furthermore, we provide evidence that, partly through its impact on precipitation, warming asymmetry is associated with a divergent response in vegetation growth.

Previous studies have detected a global trend in warming asymmetry, with the reduction in the daily temperature range being driven by strong increases in minimum temperatures in the wintertime (Easterling et al., 1997; Karl et al., 1993; Vose et al., 2005), with more extreme levels of warming having occurred towards the upper latitudes (Davy et al., 2017; Peng et al., 2013). Here we did not detect a global trend in warming asymmetry and believe that the reasons for this are twofold. First, we were interested in global trends and because seasonality varies with latitude, we used annual means and did not consider the seasonal effect. Second, because we were interested in day versus night and not maximum versus minimum temperatures, at the higher latitudes we excluded days where there was no comparative day and night, thus also controlling for seasonal variation. This explains why we did not detect the extreme warming outliers at the higher latitudes that have been reported in previous studies as this has been shown to be driven by seasonal variation with winters warming faster than summers (e.g. Hanssen-Bauer et al., 2019). At the regional level previous studies have reported diurnal asymmetry in specific humidity (Gaffen & Ross, 1999; Wang & Gaffen, 2001) and we confirm these results here.

Global patterns of diurnal temperature asymmetry and daily cloud cover were correlated (Pearson's correlation = .35). Regions where cloud cover has increased have generally experienced a larger increase of >0.25°C in night-time minimum temperatures relative to daytime maximum temperatures and this has occurred in over twice the area of land than has experienced a larger increase in daytime maximum temperatures (36.7% and 17.7% of land cover respectively). Although cloud cover is clearly a key driver of warming asymmetry, there are also other factors acting across different spatial scales that influence the daily temperature range, such as soil moisture (Dai et al., 1999) and precipitation (Dai et al., 1997; Zhou et al., 2009). We also found that there has been significant diurnal asymmetry in changing cloud cover with similar areas of land experiencing increases during the daytime or night-time, although this was only weakly correlated with warming asymmetry (Pearson's correlation = −.09). Globally, more land experienced higher specific humidity >0.1 g/m^3 and precipitation >0.1 mm/6 hr during the daytime, which is likely a result of warmer air during the day being able to hold more moisture; most of this asymmetry occurred within the tropics and subtropics. Regions where specific humidity increased more during the daytime were also more likely to experience increased night-time temperatures (Pearson's correlation = −.35). Increased daytime-specific humidity is likely a consequence of increased levels of specific humidity being capped by temperature and therefore limited when night-time temperatures are low.

Regions where night-time temperatures increased by >0.5°C more than daytime temperatures have experienced an increase in cloud cover, which has led to a trend of increasing night-time temperatures and a further wetting of the climate with increases in daytime and night-time cloud cover, specific humidity and precipitation. Through their influence on surface solar heating and upward longwave radiation, cloud cover and precipitation result in cooler days and warmer nights (Campbell & Haar, 1997; Dai et al., 1999), and these regions experienced a trend of daytime maximum temperatures remaining relatively constant while night-time minimum temperatures increased. Conversely, regions where daytime maximum temperatures increased by >0.5°C more than night-time minimum temperatures tend to be drier and experienced a reduction in cloud cover which led to a drying of the climate and twice the level of warming during the daytime while still experiencing equivalent night-time warming. Therefore, clouds can be seen primarily to act to dampen daytime maximum temperatures as opposed to increasing night-time minimum temperatures (Dai et al., 1999). At the extremes of warming asymmetry, regions which experienced night-time warming of >1°C also experienced increased specific humidity during the daytime relative to the night-time (Table S1; Figure S1). There was no diel asymmetry in cloud cover, specific humidity or precipitation at equivalent extremes of >1°C daytime warming (Table S1; Figure S1).

4.1 | Biological implications

Over half of the global land area has experienced diurnal asymmetry in warming of >0.25°C, and the direction and magnitude of this asymmetry will have profound consequences for the species inhabiting those regions and their ability to adapt in the face of the changing climate. We examined one possible biological response to

warming asymmetry, in the relationship between precipitation and vegetation growth. Night-time warming was associated with a wetting of the climate. Thus, in regions where there was a greater increase in precipitation, the associated increase in cloud cover and reduction in daytime maximum temperatures and available sunlight for photosynthesis is likely to have driven the negative association between rainfall and vegetation growth. Conversely, daytime warming was associated with a drying of the climate, and so here it is likely that water availability is the constraining factor, resulting in a positive relationship between vegetation growth and rainfall. The inherent asymmetry in change complicates predictions of ecological responses, especially in complex systems. For example, global trends in LAI are also strongly influenced by other factors, such as land use change (Hardwick et al., 2015) and local levels of CO_2 (Dermody, Long, & DeLucia, 2006; Li et al., 2018). However, their inclusion was outside of the scope of this study though likely accounts for the low explanatory power of the model ($pR^2 = .03$).

Warming asymmetry has also been found to impact the behaviour and physiology of ectotherms leading to impacts on individual fitness, species interactions and ecosystem processes (Barton & Schmitz, 2018; Speights & Barton, 2019). Regardless of whether faster warming has occurred during the daytime or night-time, regions experienced similar increases in night-time temperatures, and such hotter nights erode the ability of the night-time to act as a 'thermal refuge' where organisms can recover from daytime heat stress (Colinet, Sinclair, Vernon, & Renault, 2015; Levy, Dayan, Porter, & Kronfeld-Schor, 2019; Ma, Hoffmann, et al., 2015; Ma, Rudolf, & Ma, 2015; Zhao, Zhang, Hoffmann, & Ma, 2014). Increased daytime-specific humidity can exacerbate rising temperatures and increase the risk of heat stress in animals (Campbell & Norman, 1998), whilst increased night-time temperatures can reduce species' ability to recover. Arguably, even greater pressure is put on those species, particularly diurnal species that inhabit areas where the daytime is warming faster than the night-time. These areas also tend to be dry and are becoming drier and because increasing daytime temperatures will raise an endotherm's energy budget and increase water loss (Gardner, Peters, Kearney, Joseph, & Heinsohn, 2011), these species are also likely to become increasingly vulnerable to heat exhaustion and water loss. Furthermore, the positive difference between an endotherm's body temperature and air temperature increases with sunshine and this can exacerbate the effect because an organism's body temperature increases at a more rapid rate than air (Campbell & Norman, 1998). An increase in the frequency of extreme heat waves is likely to result in mass die offs of endotherms becoming increasingly common (McKechnie & Wolf, 2010; Welbergen, Klose, Markus, & Eby, 2008).

At the most extreme, the Tibetan Plateau (33°N, 88°E) is one of two locations (the other being the central Andes; 24°S, 68°W), with regions that have experienced a mean annual difference of >3°C between night-time minimum and daytime maximum temperatures (Table 3c; Figure 4a). The Plateau has an average elevation of 4,500 m, being the highest and largest highland in the world and rates of warming and cloud cover have been found to be significantly amplified by elevation, particularly during the night-time (Duan & Wu, 2006; Hua et al., 2018). The Plateau has also experienced diel asymmetry in the other climate variables, with increased cloud cover and some evidence of increased specific humidity at night, whilst precipitation is greater during the daytime. The Plateau has been the focus of research on the ecological impacts of warming asymmetry, primarily related to plant growth, and these impacts have been found to be diverse, from increased vegetation growth (Xia et al., 2018), shifting phenology (Liu, Yin, Shao, & Qin, 2006; Meng et al., 2019; Suonan, Classen, Zhang, & He, 2017), to reduced crop yields (Peng et al., 2004), soil respiration (Zhong, Zhang, & Zhang, 2019) and nectar yields (Mu et al., 2015). However, ecological studies have yet to consider the impacts of diel asymmetry in other aspects of the changing climate.

The biological impacts of diel asymmetry on climate are not solely dependent on the magnitude of change, but also on the latitude at which change is taking place. In tropical regions, for example, species have evolved under relatively constant and stable climatic conditions (Janzen, 1967; Sheldon, Huey, Kaspari, & Sanders, 2018), and live closer to their thermal optimum. As such, even a small temperature increase can have a large impact on their physiology, behaviour and population sizes (Deutsch et al., 2008). Projections suggest that even with <1°C of warming tropical regions will experience extreme conditions (i.e. temperatures exceeding two standard deviations from mean) sooner than other regions of the world (Beaumont et al., 2011). Therefore, we explored climatic asymmetry in two tropical regions that showed opposing directions of more extreme asymmetric warming. In West Africa (latitude 4°–14°N) night-time minimum temperatures have increased significantly more than daytime maximum temperatures, which has occurred in conjunction with a wetting of the climate (Table 3d; Figure 4b) resulting in increased vegetation growth and a reversal of desertification (Figure 5a; Herrmann, Anyamba, & Tucker, 2005). Meanwhile, in the east of the continent (latitude 12°S–7°N) warming asymmetry is reversed with daytime maximum temperatures having increased more than night-time minimum temperatures, with twice the overall levels of warming and a drying of the climate (Table 3e; Figure 4c). Increased daytime warming may help explain why climate drying has occurred, despite climate models predicting a wetting of the climate (e.g. Rowell, Booth, Nicholson, & Good, 2015). To our knowledge warming asymmetry in tropical Africa has not previously been detected due to incomplete coverage in long-term global data sets but could clearly have important implications for the ecosystems found there.

5 | CONCLUSION

In total, c. 54% of the land surface has experienced warming asymmetry of >0.25°C, and we provide further support that this is driven primarily by changing levels of cloud cover and is associated with a wetting (increased night-time warming) and drying (increased daytime warming) of the climate. Levels of night-time warming were similar regardless of whether there was greater daytime or night-time warming, indicating that increased night-time warming is largely driven by

increased cloud cover damping daytime temperatures as opposed to raising night-time temperatures (see also Dai et al., 1999). Increased night-time warming was more prevalent in wetter regions, where increased cloud cover reduces photosynthesis and drives a negative correlation between precipitation and vegetation growth. Increased daytime warming was associated with drier regions, where water availability may be the limiting factor on vegetation growth and results in a positive correlation between precipitation and vegetation growth. Diel asymmetry in how the climate is changing is likely to have major implications for temperature and water-dependent ecological processes, impacting species through thermoregulatory and water budgets. The broader implications for ectotherms and endotherms are likely to be profound. By considering climate change spatially and temporally, over the diel cycle, we can more accurately assess the climate threat posed to species, especially for those that show distinct time partitioning in biologically meaningful activities and processes.

ACKNOWLEDGEMENTS

K.J.G. was supported by a Natural Environment Research Council (NERC) grant NE/P01156X/1. A.S.G. was funded by an NERC grant NE/P01229/1 with support from the Cornwall Council.

CONFLICT OF INTEREST

The authors declare no conflict of interest.

AUTHOR CONTRIBUTION

D.T.C.C., I.M.D.M. and K.J.G. conceived and designed the study. I.M.D.M. generated the hourly climate data and the LAI layer. D.T.C.C., I.M.D.M. and A.S.G. analysed the data. D.T.C.C. and A.S.G. wrote the paper. All authors contributed critically to the drafts and gave final approval for publication of the paper. This research has not been previously presented elsewhere.

DATA AVAILABILITY STATEMENT

Data derived from public domain resources. The NCEP_Reanalysis 2 data used in this study are available from NOAA/OAR/ESRL PSD, Boulder, Colorado, United States, from their website https://www.esrl.noaa.gov/psd/. Leaf area index values are available from the National Climatic Data Center https://www.ncei.noaa.gov/data/avhrr-land-leaf-area-index-and-fapar/access/.

ORCID

Daniel T. C. Cox https://orcid.org/0000-0002-3856-3998
Ilya M. D. Maclean https://orcid.org/0000-0001-8030-9136
Alexandra S. Gardner https://orcid.org/0000-0003-3817-8982
Kevin J. Gaston https://orcid.org/0000-0002-7235-7928

REFERENCES

Alward, R. D., Detling, J. K., & Milchunas, D. G. (1999). Grassland vegetation changes and nocturnal global warming. *Science*, *283*(5399), 229–231. https://doi.org/10.1126/science.283.5399.229

Asner, G. P., Braswell, B. H., Schimel, D. S., & Wessman, C. A. (1998). Ecological research needs from multiangle remote sensing data. *Remote Sensing of Environment*, *63*, 155–165. https://doi.org/10.1016/S0034-4257(97)00139-9

Atkin, O. K., Turnbull, M. H., Zaragoza-Castells, K., Fyllas, N. M., Lloyd, J., Meir, P., & Griffin, K. L. (2013). Light inhibition of leaf respiration as soil fertility declines along a post-glacial chronosequence in New Zealand: An analysis using the Kok method. *Plant and Soil*, *367*, 163–182. https://doi.org/10.1007/s11104-013-1686-0

Barton, B. T., & Schmitz, O. J. (2018). Opposite effects of daytime and nighttime warming on top-down control of plant diversity. *Ecology*, *99*(1), 13–20. https://doi.org/10.1002/ecy.2062

Beaumont, L. J., Pitman, A., Perkins, S., Zimmermann, N. E., Yoccoz, N. G., & Thuiller, W. (2011). Impacts of climate change on the world's most exceptional ecoregions. *Proceedings of the National Academy of Sciences of the United States of America*, *108*(6), 2306–2311. https://doi.org/10.1073/pnas.1007217108

Beier, C., Emmett, B. A., Penuelas, J., Schmidt, I. K., Tietema, A., Estiarte, M., … Gorissen, A. (2008). Carbon and nitrogen cycles in European ecosystems respond differently to global warming. *Science of the Total Environment*, *407*, 692–697. https://doi.org/10.1016/j.scitotenv.2008.10.001

Bennie, J. J., Duffy, J. P., Inger, R., & Gaston, K. J. (2014). Biogeography of time partitioning in mammals. *Proceedings of the National Academy of Sciences of the United States of America*, *111*(38), 13727–13732. https://doi.org/10.1073/pnas.1216063110

Boussetta, S., Balsamo, G., Beljaars, A., Kral, T., & Jarlan, L. (2013). Impact of a satellite-derived lead area index monthly climatology in a global numerical weather prediction model. *International Journal of Remote Sensing*, *34*, 3520–3542. https://doi.org/10.1080/01431161.2012.716543

Brodzik, M. J., Billingsley, B., Haran, T., Raup, B., & Savoie, M. H. (2012). EASE-Grid 2.0: incremental but significant improvements for earth-gridded data sets. *ISPRS International Journal of Geo-Information*, *1*(1), 32–45. https://doi.org/10.3390/ijgi1010032

Campbell, G. G., & Haar, T. H. V. (1997). Comparison of surface temperature minimum and maximum and satellite measured cloudiness and radiation budget. *Journal of Geophysical Research: Atmospheres*, *102*(D14), 16639–16645. https://doi.org/10.1029/96JD02718

Campbell, G. S., & Norman, J. N. (1998). Animals and their environment. In G. S. Campbell & J. N. Norman (Eds.), *An introduction to environmental biophysics* (pp. 185–207). New York, NY: Springer.

Chen, L., & Dirmeyer, P. A. (2019). The relative importance among anthropogenic forcings of land use/land cover change in affecting temperature extremes. *Climate Dynamics*, *52*(3–4), 2269–2285. https://doi.org/10.1007/s00382-018-4250-z

Colinet, H., Sinclair, B. J., Vernon, P., & Renault, D. (2015). Insects in fluctuating thermal environments. *Annual Review of Entomology*, *60*(1), 123–140. https://doi.org/10.1146/annurev-ento-010814-021017

Dai, A., Genio, A. D. D., & Fung, I. Y. (1997). Clouds, precipitation and temperature range. *Nature*, *386*, 665. https://doi.org/10.1038/386665b0

Dai, A., Trenberth, K. E., & Karl, T. R. (1999). Effects of clouds, soil moisture, precipitation, and water vapor on diurnal temperature range. *Journal of Climate*, *12*(8), 2451–2473. https://doi.org/10.1175/1520-0442(1999)012<2451:EOCSMP>2.0.CO;2

Davy, R., Esau, I., Chernokulsky, A., Outten, S., & Zilitinkevich, S. (2017). Diurnal asymmetry to the observed global warming. *International Journal of Climatology*, *37*(1), 79–93. https://doi.org/10.1002/joc.4688

Dermody, O., Long, S. P., & DeLucia, E. H. (2006). How does elevated CO_2 or ozone affect the leaf-area index of soybean when applied independently? *New Phytologist*, *169*(1), 145–155. https://doi.org/10.1111/j.1469-8137.2005.01565.x

Deutsch, C. A., Tewksbury, J. J., Huey, R. B., Sheldon, K. S., Ghalambor, C. K., Haak, D. C., & Martin, P. R. (2008). Impacts of climate warming on terrestrial ectotherms across latitude. *Proceedings of the National Academy of Sciences of the United States of America*, *105*(18), 6668–6672. https://doi.org/10.1073/pnas.0709472105

Donat, M. G., & Alexander, L. V. (2012). The shifting probability distribution of global daytime and night-time temperatures. *Geophysical Research Letters*, *39*(14), L14707. https://doi.org/10.1029/2012GL052459

Du, H., Wu, Z., Jin, Y., Zong, S., & Meng, X. (2013). Quantitative relationships between precipitation and temperature over Northeast China, 1961–2010. *Theoretical and Applied Climatology*, *113*(3), 659–670. https://doi.org/10.1007/s00704-012-0815-7

Duan, A., & Wu, G. (2006). Change of cloud amount and the climate warming on the Tibetan Plateau. *Geophysical Research Letters*, *33*(22), L22704. https://doi.org/10.1029/2006GL027946

Easterling, D. R., Horton, B., Jones, P. D., Peterson, T. C., Karl, T. R., Parker, D. E., … Folland, C. K. (1997). Maximum and minimum temperature trends for the globe. *Science*, *277*(5324), 364. https://doi.org/10.1126/science.277.5324.364

Gaffen, D. J., & Ross, R. J. (1999). Climatology and trends of U.S. surface humidity and temperature. *Journal of Climate*, *12*(3), 811–828. https://doi.org/10.1175/1520-0442(1999)012<0811:CATOUS>2.0.CO;2

Gardner, J. L., Peters, A., Kearney, M. R., Joseph, L., & Heinsohn, R. (2011). Declining body size: A third universal response to warming? *Trends in Ecology & Evolution*, *26*(6), 285–291. https://doi.org/10.1016/j.tree.2011.03.005

Hanssen-Bauer, I., Førland, E. J., Hisdal, H., Mayer, S., Sandø, A. B., & Sorteberg, A. (2019). Climate in Svalbard 2100 – A knowledge base for climate adaptation. The Norwegian Centre for Climate Services. Retrieved from https://www.miljodirektoratet.no/globalassets/publikasjoner/M1242/M1242.pdf

Hardwick, S. R., Toumi, R., Pfeifer, M., Turner, E. C., Nilus, R., & Ewers, R. M. (2015). The relationship between leaf area index and microclimate in tropical forest and oil palm plantation: Forest disturbance drives changes in microclimate. *Agricultural and Forest Meteorology*, *201*, 187–195. https://doi.org/10.1016/j.agrformet.2014.11.010

Herrmann, S. M., Anyamba, A., & Tucker, C. J. (2005). Recent trends in vegetation dynamics in the African Sahel and their relationship to climate. *Global Environmental Change*, *15*, 394–404. https://doi.org/10.1016/j.gloenvcha.2005.08.004

Hijmans, R. J. (2019). *raster: Geographic Data Analysis and Modelling*. R package version 2.8-19. [Computer software]. Retrieved from https://CRAN.R-project.org/package=raster

Hua, S., Liu, Y., Jia, R., Chang, S., Wu, C., Zhu, Q., … Wang, B. (2018). Role of clouds in accelerating cold-season warming during 2000–2015 over the Tibetan Plateau. *International Journal of Climatology*, *38*(13), 4950–4966. https://doi.org/10.1002/joc.5709

Huntington, T. G. (2006). Evidence for intensification of the global water cycle: Review and synthesis. *Journal of Hydrology*, *319*(1), 83–95. https://doi.org/10.1016/j.jhydrol.2005.07.003

IPCC. (2013). Summary for policymakers. In T. F. Stocker, D. Qin, G.-K. Plattner, M. Tignor, S. K. Allen, J. Boschung, A. Nauels, Y. Xia, V. Bex, & P. M. Midgley (Eds.), *Climate change 2013: The physical science basis Contribution of working group I to the fifth assessment report of the intergovernmental panel on climate change* (pp. 37–38). Cambridge and New York, NY: Cambridge University Press.

Janzen, D. H. (1967). Why mountain passes are higher in the tropics. *The American Naturalist*, *101*(919), 233–249. https://doi.org/10.1086/282487

Jarlan, L., Balsamo, G., Lafont, S., Beljaars, A., Calvet, J. C., & Mougin, E. (2008). Analysis of leaf area index in the ECMWF land surface model and impact on latent heat and carbon fluxes: Application to West Africa. *Journal of Geophysical Research*, *113*, D24117. https://doi.org/10.1029/2007JD009370

Karl, T. R., Jones, P. D., Knight, R. W., Kukla, G., Plummer, N., Razuvayev, V., … Peterson, T. C. (1993). A new perspective on recent global warming: Asymmetric trends of daily maximum and minimum temperature. *Bulletin of the American Meteorological Society*, *74*(6), 1007–1024. https://doi.org/10.1175/1520-0477(1993)074<1007:ANPORG>2.0.CO;2

Karl, T. R., Kukla, G., Razuvayev, V. N., Changery, M. J., Quayle, R. G., Heim, R. R., … Fu, C. B. (1991). Global warming – Evidence for asymmetric diurnal temperature-change. *Geophysical Research Letters*, *18*(12), 2253–2256. https://doi.org/10.1029/91gl02900

Kuang, X., & Jiao, J. J. (2016). Review on climate change on the Tibetan Plateau during the last half century. *Journal of Geophysical Research: Atmospheres*, *121*(8), 3979–4007. https://doi.org/10.1002/2015JD024728

Lamarche, C., Santoro, M., Bontemps, S., d'Andrimont, R., Radoux, J., Giustarini, L., … Arino, O. (2017). Compilation and validation of SAR and optical data products for a complete and global map of inland/ocean water tailored to the climate modelling community. *Remote Sensing*, *9*(1), 36. https://doi.org/10.3390/rs9010036

Lee, X., Goulden, M. L., Hollinger, D. Y., Barr, A., Black, T. A., Bohrer, G., … Zhao, L. (2011). Observed increase in local cooling effect of deforestation at higher latitudes. *Nature*, *479*, 384. https://doi.org/10.1038/nature10588

Levy, O., Dayan, T., Porter, W. P., & Kronfeld-Schor, N. (2019). Time and ecological resilience: Can diurnal animals compensate for climate change by shifting to nocturnal activity? *Ecological Monographs*, *89*(1), e01334. https://doi.org/10.1002/ecm.1334

Li, Q., Lu, X., Wang, Y., Huang, X., Cox, P. M., & Luo, Y. (2018). Leaf area index as identified as a major source of variability in modelled CO_2 fertilization. *Biogeosciences*, *15*, 6909–6925. https://doi.org/10.5194/bg-15-6909-2018

Liu, X., Yin, Z.-Y., Shao, X., & Qin, N. (2006). Temporal trends and variability of daily maximum and minimum, extreme temperature events, and growing season length over the eastern and central Tibetan Plateau during 1961–2003. *Journal of Geophysical Research: Atmospheres*, *111*(D19), 1961–2003. https://doi.org/10.1029/2005JD006915

Ma, G., Hoffmann, A. A., & Ma, C.-S. (2015). Daily temperature extremes play an important role in predicting thermal effects. *Journal of Experimental Biology*, *218*(14), 2289–2296. https://doi.org/10.1242/jeb.122127

Ma, G., Rudolf, V. H. W., & Ma, C. (2015). Extreme temperature events alter demographic rates, relative fitness, and community structure. *Global Change Biology*, *21*(5), 1794–1808. https://doi.org/10.1111/gcb.12654

Maclean, I. M. D., Mosedale, J. R., & Bennie, J. J. (2019). Microclima: An R package for modelling meso- and microclimate. *Methods in Ecology and Evolution*, *10*, 280–290. https://doi.org/10.1111/2041-210X.13093

Maclean, I. M. D., Suggitt, A. J., Wilson, R. J., Duffy, J. P., & Bennie, J. J. (2017). Fine-scale climate change: Modelling spatial variation in biologically meaningful rates of warming. *Global Change Biology*, *23*(1), 256–268. https://doi.org/10.1111/gcb.13343

Maclean, I. M. D., & Wilson, R. J. (2011). Recent ecological responses to climate change support predictions of high extinction risk. *Proceedings of the National Academy of Sciences of the United States of America*, *108*(30), 12337–12342. https://doi.org/10.1073/pnas.1017352108

McKechnie, A. E., & Wolf, B. O. (2010). Climate change increases the likelihood of catastrophic avian mortality events during extreme heat waves. *Biology Letters*, *6*(2), 253–256. https://doi.org/10.1098/rsbl.2009.0702

Meng, F., Zhang, L., Niu, H., Suonan, J., Zhang, Z., Wang, Q., … Du, M. (2019). Divergent responses of community reproductive and vegetative phenology to warming and cooling: Asymmetry versus symmetry. *Frontiers in Plant Science*, *10*. https://doi.org/10.3389/fpls.2019.01310

Mu, J., Peng, Y., Xi, X., Wu, X., Li, G., Niklas, K. J., & Sun, S. (2015). Artificial asymmetric warming reduces nectar yield in a Tibetan alpine species of Asteraceae. *Annals of Botany*, *116*(6), 899–906. https://doi.org/10.1093/aob/mcv042

Ohmura, A., & Wild, M. (2002). Is the hydrological cycle accelerating? *Science*, *298*(5597), 1345–1346. https://doi.org/10.1126/science.1078972

Peng, S. B., Huang, J. L., Sheehy, J. E., Laza, R. C., Visperas, R. M., Zhong, X. H., … Cassman, K. G. (2004). Rice yields decline with higher night temperature from global warming. *Proceedings of the National Academy of Sciences of the United States of America*, *101*(27), 9971–9975. https://doi.org/10.1073/pnas.0403720101

Peng, S., Piao, S., Ciais, P., Myneni, R. B., Chen, A., Chevallier, F., … Zeng, H. (2013). Asymmetric effects of daytime and night-time warming on Northern Hemisphere vegetation. *Nature*, *501*(7465), 88–92. https://doi.org/10.1038/nature12434

Peraudeau, S., Roques, S., Quiñones, C. O., Fabre, D., Van Rie, J., Ouwerkerk, P. B. F., … Lafarge, T. (2015). Increase in night temperature in rice enhances respiration rate without significant impact on biomass accumulation. *Field Crops Research*, *171*, 67–78. https://doi.org/10.1016/j.fcr.2014.11.004

Pielke, R. A. (2005). Land use and climate change. *Science*, *310*(5754), 1625–1626. https://doi.org/10.1126/science.1120529

Pingale, S., Adamowski, J., Jat, M., & Khare, D. (2015). Implications of spatial scale on climate change assessments. *Journal of Water and Land Development*, *26*(1), 37–55. https://doi.org/10.1515/jwld-2015-0015

QGIS Development Team. (2018). QGIS Geographic Information System. Open Source Geospatial Foundation Project. Version 3.4.1. http://qgis.osgeo.org

R Core Team. (2018). *R: A language and environment for statistical computing*. Vienna, Austria: R foundation for Statistical Computing. Retrieved from http://www.Rproject.org/

Rangwala, I., Sinsky, E., & Miller, J. R. (2013). Amplified warming projections for high altitude regions of the northern hemisphere mid-latitudes from CMIP5 models. *Environmental Research Letters*, *8*(2), 024040. https://doi.org/10.1088/1748-9326/8/2/024040

Rowell, D. P., Booth, B. B. B., Nicholson, S., & Good, P. (2015). Reconciling past and future rainfall trends over East Africa. *Journal of Climate*, *28*, 9768–9788. https://doi.org/10.1175/JCLI-D-15-0140.1

Sheldon, K. S., Huey, R. B., Kaspari, M., & Sanders, N. J. (2018). Fifty years of mountain passes: A perspective on Dan Janzen's classic article. *The American Naturalist*, *191*(5), 553–565. https://doi.org/10.1086/697046

Speights, C. J., & Barton, B. T. (2019). Timing is everything: Effects of day and night warming on predator functional traits. *Food Webs*, *21*, e00130. https://doi.org/10.1016/j.fooweb.2019.e00130

Suggitt, A. J., Wilson, R. J., Isaac, N. J. B., Beale, C. M., Auffret, A. G., August, T., … Maclean, I. M. D. (2018). Extinction risk from climate change is reduced by microclimatic buffering. *Nature Climate Change*, *8*(8), 713–717. https://doi.org/10.1038/s41558-018-0231-9

Sun, B., Groisman, P. Y., Bradley, R. S., & Keimig, F. T. (2000). Temporal changes in the observed relationship between cloud cover and surface air temperature. *Journal of Climate*, *13*(24), 4341–4357. https://doi.org/10.1175/1520-0442(2000)013<4341:TCITOR>2.0.CO;2

Suonan, J., Classen, A. T., Zhang, Z., & He, J. S. (2017). Asymmetric winter warming advanced plant phenology to a greater extent than symmetric warming in an alpine meadow. *Functional Ecology*, *31*, 2147–2156. https://doi.org/10.1111/1365-2435.12909

Sutton, R., Suckling, E., & Hawkins, E. (2015). What does global mean temperature tell us about local climate? *Philosophical Transactions of the Royal Society A*, *373*(2054), 20140426. https://doi.org/10.1098/rsta.2014.0426

Vermote, E., & NOAA CDR Program. (2019). *NOAA Climate Data Record (CDR) of AVHRR Leaf Area Index (LAI) and Fraction of Absorbed Photosynthetically Active Radiation (FAPAR), Version 5*. NOAA National Centers for Environmental Information. Retrieved from https://doi.org/10.7289/V5TT4P69

Vose, R. S., Easterling, D. R., & Gleason, B. (2005). Maximum and minimum temperature trends for the globe: An update through 2004. *Geophysical Research Letters*, *32*(23), L23822. https://doi.org/10.1029/2005GL024379

Walther, G.-R., Post, E., Convey, P., Menzel, A., Parmesan, C., Beebee, T. J. C., … Bairlein, F. (2002). Ecological responses to recent climate change. *Nature*, *416*(6879), 389. https://doi.org/10.1038/416389a

Wan, S., Xia, J., Liu, W., & Niu, S. (2009). Photosynthetic overcompensation under nocturnal warming enhances grassland carbon sequestration. *Ecology*, *90*, 2700–2710. https://doi.org/10.1890/08-2026.1

Wang, J. X. L., & Gaffen, D. J. (2001). Late-twentieth-century climatology and trends of surface humidity and temperature in China. *Journal of Climate*, *14*(13), 2833–2845. https://doi.org/10.1175/1520-0442(2001)014<2833:LTCCAT>2.0.CO;2

Welbergen, J. A., Klose, S. M., Markus, N., & Eby, P. (2008). Climate change and the effects of temperature extremes on Australian flying-foxes. *Proceedings of the Royal Society B*, *275*(1633), 419–425. https://doi.org/10.1098/rspb.2007.1385

Xia, H., Li, A., Feng, G., Li, Y., Qin, Y., Lei, G., & Cui, Y. (2018). The effects of asymmetric diurnal warming on vegetation growth of the Tibetan Plateau over the past three decades. *Sustainability*, *10*(4), 1103. https://doi.org/10.3390/su10041103

Xia, J., Chen, J., Piao, S., Ciais, P., Luo, Y., & Wan, S. (2014). Terrestrial carbon cycle affected by non-uniform climate warming. *Nature Geoscience*, *7*(3), 173–180. https://doi.org/10.1038/ngeo2093

Xu, X., Medvigy, D., Powers, J. S., Becknell, J. M., & Guan, K. (2016). Diversity in plant hydraulic traits explains seasonal and inter-annual variations of vegetation dynamics in seasonally dry tropical forests. *New Phytologist*, *212*(1), 80–95. https://doi.org/10.1111/nph.14009

Zhao, F., Zhang, W., Hoffmann, A. A., & Ma, C.-S. (2014). Night warming on hot days produces novel impacts on development, survival and reproduction in a small arthropod. *Journal of Animal Ecology*, *83*(4), 769–778. https://doi.org/10.1111/1365-2656.12196

Zhong, Z., Zhang, G., & Zhang, H. (2019). Impact of diurnal unsymmetrical warming on soil respiration in an agroecological system of the Lhasa region. *PLoS ONE*, *14*(5), e0217575. https://doi.org/10.1371/journal.pone.0217575

Zhou, L. M., Chen, H. S., & Dai, Y. J. (2015). Stronger warming amplification over drier ecoregions observed since 1979. *Environmental Research Letters*, *10*(6), 064012. https://doi.org/10.1088/1748-9326/10/6/064012

Zhou, L., Dai, A., Dai, Y., Vose, R. S., Zou, C.-Z., Tian, Y., & Chen, H. (2009). Spatial dependence of diurnal temperature range trends on precipitation from 1950 to 2004. *Climate Dynamics*, *32*(2), 429–440. https://doi.org/10.1007/s00382-008-0387-5

SUPPORTING INFORMATION

Additional supporting information may be found online in the Supporting Information section.

How to cite this article: Cox DTC, Maclean IMD, Gardner AS, Gaston KJ. Global variation in diurnal asymmetry in temperature, cloud cover, specific humidity and precipitation and its association with leaf area index. *Glob Change Biol*. 2020;00:1–13. https://doi.org/10.1111/gcb.15336